Vol 14 No 6, June 2005
1009-1963/2005/14(06)/1185-08

Chinese Physics

© 2005 Chin. Phys. Soc.
and IOP Publishing Ltd

New equation of turbulent fibre suspensions and its solution and application to the pipe flow*

Lin Jian-Zhong(林建忠)[a)†], Li Jun(李 俊)[a)],
Zhu Li(朱 力)[a)], and James A. Olson[b)]

[a)] *Department of Mechanics, State Key Laboratory of Fluid Power Transmission and Control, Zhejiang University, Hangzhou 310027, China*

[b)] *Department of Mechanical Engineering, Pulp and Paper Center, The University of British Columbia, Vancouver, BC, V6T 1Z4 Canada*

(Received 29 October 2004; revised manuscript received 17 February 2005)

The mean motion equation of turbulent fibre suspensions and the equation of probability distribution function for mean fibre orientation are derived. The successive iteration for calculating the mean orientation distribution of fibres and the mean and fluctuation-correlated quantities of suspensions is presented. The equations and their solutions are applied to a turbulent pipe flow of fibre suspensions, and a corresponding experiment is performed. It is found that the theoretical and experimental results are in good agreement with each other. The obtained results for turbulent pipe flow of fibre suspensions show that the flow rate of fibre suspensions is large under the same pressure drop in comparison with the rate of Newtonian flow in the absence of fibre suspensions. Fibres play an important role in reducing the flow drag. The amount of reduction in drag augments with the increase of the concentration of the fibre mass. The relative turbulent intensity and Reynolds stress in the fibre suspensions are smaller than those in the Newtonian flow under the same condition, which illustrates that the fibres have an influence on suppressing the turbulence. The amount of suppression is directly proportional to the concentration of the fibre mass.

Keywords: fibre suspension, turbulent pipe flow
PACC: 4755K, 4750, 4725J, 4760

1. Introduction

It is found that fibre suspensions have more and more applications in a variety of industries such as the composite manufacturing, environmental, chemical, and textile engineering, and paper making. The characteristics of the flow play an important role in the quality of product

Different from spherical particles, the fibres with non-isotropic shapes in suspensions have a great influence on the fluid even at very low concentrations. The spatial and orientational distributions of fibres depend on the motion of the fluid. Despite many investigations into laminar fibre suspensions already made, the behaviours of turbulent fibre suspensions commonly used in engineering are still not well understood because of the difficulties in both turbulence and motion of the fibres. There exists some literature dealing with the turbulent fibre suspensions. Asgharian and Yu[1] investigated the glass fibre deposition onto human lung trachea. Kagermann and Kohler[2] studied the rotational and translational dispersion of fibres in a turbulent flow by assuming the dimension of fibres to be less than that of smallest eddies in the flow. Krushkal and Gallily[3] calculated the orientation distribution function of fibres by use of the Fokker–Planck equation in a turbulent flow. Olson and Kerekes[4,5] obtained the translational and rotational dispersion coefficients on the assumption that the relative velocity between particle and fluid could be neglected. Lin *et al* studied the orientation distribution of fibres respectively in a mixing layer with coherent structures[6] and in a turbulent pipe flow.[7] Gao and Lin[8] derived the translational and rotational dispersion coefficients of fibres with the balance between the Stokes drag and virtual mass force taken into consideration, and discussed the dispersion prop-

*Project supported by the National Natural Science Foundation of China (Grant No 10372090) and the Doctoral Program of Higher Education of China (Grant No 20030335001).

†E-mail: jzlin@sfp.zju.edu.cn

erty of fibres, long and short. The above investigations, however, focused only on the orientation distribution of fibres in the turbulent flows, bud not on the turbulent property of the fibre suspensions. Lin *et al*[9] investigated the effect of fibres on the turbulent property of flow, but only one-way coupling approach was used, that is, the effect of the fluid on the fibres was neglected. In order to consider the interaction between fluid and fibre, the relevant equations should be built up.

The flow is complicated when the interaction between fluid and fibre is present, and even more complicated if it is turbulent. Consequently, the mean motion equation of turbulent fibre suspensions, including the Reynolds stress and the effects of fibres, and the equation of probability distribution function for mean fibre orientation including the fluctuating correlation have not been reported up to now. Therefore, the aim of this study is to derive the above equations and their solutions, and verify these equations and their solutions by applying them to a turbulent pipe flow of fibre suspensions.

2. Derivation of the basic equations

2.1. Instantaneous motion equation of fibre suspensions

A fluid is assumed to be incompressible, the instantaneous continuity and motion equations of fibre suspensions, respectively, are[10]

$$\frac{\partial u_i}{\partial x_i} = 0, \tag{1}$$

$$\frac{\partial u_i}{\partial t} + u_j \frac{\partial u_i}{\partial x_j} = -\frac{1}{\rho}\frac{\partial p}{\partial x_i} + \nu \frac{\partial^2 u_i}{\partial^2 x_j} + \frac{\mu_f}{\rho}\frac{\partial}{\partial x_j} \times \left[a_{ijkl}\varepsilon_{kl} - \frac{1}{3}(I_{ij}a_{kl})\varepsilon_{kl}\right], \tag{2}$$

where u_i is the velocity, p the pressure, ν the kinematical viscosity of the suspending fluid, ε_{ij} the tensor of strain rate, $\varepsilon_{ij} = (\partial u_i/\partial x_j + \partial u_j/\partial x_i)/2$, μ_f the apparent viscosity of the suspensions. The complexity of fibre suspensions results from the effects of particle-particle[11,12] and particle-solvent[13] in the third term on the right-hand side of Eq.(2). For a semi-dilute suspension, μ_f is given by[14]

$$\mu_f = \frac{\pi n L^3 \mu}{3\left[\lg(1/c) + \lg\lg(1/c) + A(c)\right]}, \tag{3}$$

where n is the number of fibres per unit volume, L and d the length and the diameter of the fibres, respectively, μ the dynamical viscosity of the suspending fluid, c the volume fraction of the fibres, $c = (\pi/4)nLd^2$, $A(c)$ is a constant and equals -0.663 in general.

The second- and fourth-orientation tensors of the fibre, a_{kl} and a_{ijkl}, in Eq.(2) are defined respectively by[15,16]

$$a_{ij} = \oint p_i p_j \psi(\boldsymbol{p})\,\mathrm{d}\boldsymbol{p}, \tag{4}$$

$$a_{ijkl} = \oint p_i p_j p_k p_l \psi(\boldsymbol{p})\,\mathrm{d}\boldsymbol{p}, \tag{5}$$

where p_i is a unit vector parallel to the fibre's axis of symmetry, $\psi(\boldsymbol{p})$ the probability distribution function for fibre orientation at any position in the flow.

2.2. Instantaneous equation of probability distribution function for fibre orientation

$\psi(\boldsymbol{p})$ is the probability distribution function for fibre orientation, then $\psi(\boldsymbol{p})\,\mathrm{d}\boldsymbol{p}$ is the probability that the fibre orientation is located between $\boldsymbol{p}$ and $(\boldsymbol{p} + \mathrm{d}\boldsymbol{p})$. $\psi(\boldsymbol{p})$ satisfies the following condition of conservation:

$$\frac{\partial \psi}{\partial t} + u_j \frac{\partial \psi}{\partial x_j} = -\frac{\partial(\psi \dot{p}_j)}{\partial p_j}, \tag{6}$$

where $\dot{p}_j$ is the angular velocity of fibre. Neglecting the orientation dispersion resulting from the hydrodynamic interaction between the fibres, $\dot{p}_i$ is given by[17]

$$\dot{p}_i = -\omega_{ij}p_j + \lambda\varepsilon_{ij}p_j - \lambda\varepsilon_{kl}p_k p_l p_i, \tag{7}$$

where ω_{ij} is the vorticity tensor, $\omega_{ij} = (\partial u_j/\partial x_i - \partial u_i/\partial x_j)/2$, and the parameter$\lambda = \left(r^2-1\right)/\left(r^2+1\right)$ with r being the aspect ratio of fibre.

2.3. Mean motion equation of turbulent fibre suspensions

Expressing the instantaneous quantities of velocity, pressure, tensor of strain rate and orientation tensor in Eq.(2) respectively as the sum of the mean and fluctuating quantities yields

$$\begin{aligned} &u_i = \bar{u}_i + u_i'; \quad p = \overline{p} + p';\\ &\varepsilon_{ij} = \overline{\varepsilon_{ij}} + \varepsilon_{ij}'; \quad a_{ij} = \overline{a_{ij}} + a_{ij}';\\ &a_{ijkl} = \overline{a_{ijkl}} + a_{ijkl}'. \end{aligned} \tag{8}$$

Because a_{ijkl}' and a_{ij}' are the variables depending on the rotation angle of the fibre, while ε_{ij}' is the variable depending on the specific position of the fibre. The correlations of $\overline{a_{ijkl}'\varepsilon_{kl}'}$ and $\overline{a_{kl}'\varepsilon_{kl}'}$ are equal

to zero. Substituting Eq.(8) into Eq.(2) and taking the average over the terms in the equation, we have

$$\frac{\partial \bar{u}_i}{\partial t} + \bar{u}_j \frac{\partial \bar{u}_i}{\partial x_j} = -\frac{1}{\rho}\frac{\partial \overline{p}}{\partial x_i} + \nu \frac{\partial^2 \bar{u}_i}{\partial^2 x_j} - \frac{\partial \overline{u_i' u_j'}}{\partial x_j} + \frac{\mu_f}{\rho}\frac{\partial}{\partial x_j}\left(\overline{a_{ijkl}\varepsilon_{kl}} - \frac{1}{3} I_{ij}\overline{a_{klpq}\varepsilon_{kl}}\right). \tag{9}$$

This is the mean motion equation of turbulent fibre suspensions.

2.4. Equation of probability distribution function for mean fibre orientation

Expressing the instantaneous quantities of velocity, probability distribution function, and angular velocity for fibre in Eq.(6) respectively as the sum of the mean and fluctuating quantities, we have

$$u_i = \bar{u}_i + u_i', \quad \psi = \bar{\psi} + \psi', \quad \dot{p}_i = \bar{\dot{p}}_i + \dot{p}_i'. \tag{10}$$

Substituting Eq.(10) into Eq.(6) and taking the average over the terms in the equation, then combining the continuity equation (1), we have

$$\frac{\partial \bar{\psi}}{\partial t} + \bar{u}_j \frac{\partial \bar{\psi}}{\partial x_j} + \frac{\partial\left(\bar{\psi}\bar{\dot{p}}_j\right)}{\partial p_j} = -\overline{\frac{\partial u_j' \psi'}{\partial x_j}} - \overline{\frac{\partial\left(\psi' \dot{p}_j'\right)}{\partial p_j}}, \tag{11}$$

where the term $-\overline{u_j'\psi'}$ is the correlation of the fluctuating velocity with the fluctuating probability distribution function, and the term $\overline{\psi'\dot{p}_j'}$ is the correlation of the fluctuating rotation angular velocity with the fluctuating probability distribution function. These two terms can be expressed by the mean quantities

$$-\overline{\psi' u_j'} = \alpha_{\psi x}\frac{\partial \overline{\psi}}{\partial x_j} \quad \text{and} \quad -\overline{\psi'\dot{p}_j'} = \alpha_{\psi p}\frac{\partial \overline{\psi}}{\partial p_j}, \tag{12}$$

where $\alpha_{\psi x}$ and $\alpha_{\psi p}$ are the dispersion coefficients of linear and angular displacements, respectively. Substituting Eq.(12) into Eq.(11), we have

$$\frac{\partial \bar{\psi}}{\partial t} + \bar{u}_j \frac{\partial \bar{\psi}}{\partial x_j} + \frac{\partial\left(\bar{\psi}\bar{\dot{p}}_j\right)}{\partial p_j} = \alpha_{\psi x}\frac{\partial^2 \overline{\psi}}{\partial x_j^2} + \alpha_{\psi p}\frac{\partial^2 \overline{\psi}}{\partial p_j^2}. \tag{13}$$

The angular velocity of the fibre's rotation in Eq.(13) can be derived from Eq.(7). Therefore, after expressing the instantaneous angular velocity of rotation, vorticity tensor of the flow, and tensor of rate of strain in Eq.(7) respectively as the sum of the mean and fluctuation quantities, then substituting them into Eq.(7) and taking average, we have

$$\bar{\dot{p}}_i = -\bar{\omega}_{ij} p_j + \lambda \overline{\varepsilon_{ij}} p_j - \lambda \overline{\varepsilon_{kl}} p_k p_l p_i. \tag{14}$$

Substituting Eq.(14) into Eq.(13), we have

$$\frac{\partial \bar{\psi}}{\partial t} + \bar{u}_j \frac{\partial \bar{\psi}}{\partial x_j} + \frac{\partial[\bar{\psi}(-\bar{\omega}_{ji} p_i + \lambda \overline{\varepsilon_{ji}} p_i - \lambda \overline{\varepsilon_{kl}} p_k p_l p_j)]}{\partial p_j} = \alpha_{\psi x}\frac{\partial^2 \overline{\psi}}{\partial x_j^2} + \alpha_{\psi p}\frac{\partial^2 \overline{\psi}}{\partial p_j^2}. \tag{15}$$

Because $\overline{\omega}_{ii} = 0$ and $\overline{\varepsilon_{ii}} = 0$ for the incompressible flow, we can expand Eq.(15) as

$$\frac{\partial \bar{\psi}}{\partial t} + \bar{u}_j \frac{\partial \bar{\psi}}{\partial x_j} - \bar{\omega}_{ji} p_i \frac{\partial \bar{\psi}}{\partial p_j} + \lambda \overline{\varepsilon_{ji}} p_i \frac{\partial \bar{\psi}}{\partial p_j} - \lambda \overline{\varepsilon_{kl}} p_k p_l p_j \frac{\partial \bar{\psi}}{\partial p_j} - \lambda \overline{\varepsilon_{kl}} \bar{\psi} p_k p_l = \alpha_{\psi x}\frac{\partial^2 \overline{\psi}}{\partial x_j^2} + \alpha_{\psi p}\frac{\partial^2 \overline{\psi}}{\partial p_j^2}. \tag{16}$$

This is the equation of probability distribution function for mean fibre orientation.

$\overline{a_{ij}}$ and $\overline{a_{ijkl}}$ can be obtained by substituting $\bar{\psi}$ into Eqs.(4) and (5):

$$\overline{a_{ij}} = \oint p_i p_j \overline{\psi(\boldsymbol{p})} \mathrm{d}\boldsymbol{p}, \tag{17}$$

$$\overline{a_{ijkl}} = \oint p_i p_j p_k p_l \overline{\psi(\boldsymbol{p})} \mathrm{d}\boldsymbol{p}. \tag{18}$$

3. Successive iteration

The basic equations of turbulent fibre suspensions consist of Eqs.(9), (16), (17) and (18). By solving these equations, we can obtain the probability distribution function and the second- and fourth-orientation tensors for mean fibre orientation, the additional stress induced by the fibres, the mean velocity, the turbulent intensity and the Reynolds stress of suspensions.

It is difficult, however, to solve the above coupled equations in one or several time steps. For this reason we present a successive iteration as follows:

(i) Take the velocity $\bar{u}_i^0$, vorticity $\overline{\omega_{ij}}^0$ and rate of strain $\overline{\varepsilon_{ij}}^0$ for the Newtonian fluid without fibre as the zero-order approximation solutions.

(ii) Substitute the zero-order approximation solutions $\bar{u}_i^0$, $\overline{\omega_{ij}}^0$, $\overline{\varepsilon_{ij}}^0$ into Eq.(16), and obtain the zero-order approximation solution $\bar{\psi}^0$ of the probability distribution function for mean fibre orientation by solving Eq.(16).

(iii) Substitute $\bar{\psi}^0$ into Eqs.(17) and (18), and obtain the zero-order approximation solutions $\overline{a_{ij}}^0$ and $\overline{a_{ijkl}}^0$ of the second- and fourth-orientation tensors for mean fibre orientation.

(iv) Substitute $\overline{a_{ij}}^0$, $\overline{a_{ijkl}}^0$ and $\overline{\varepsilon_{ij}}^0$ into Eq.(9), and obtain the first-order approximation solution of mean velocity $\bar{u}_i^1$, turbulent intensity and Reynolds stress $\overline{u_i' u_j'}^1$ by solving Eq.(9) together with the closure model of turbulence.

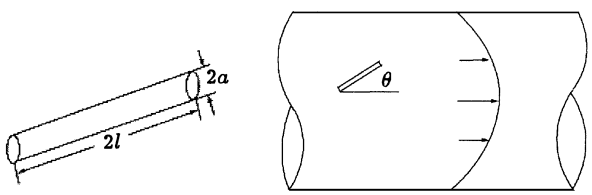
(v) Calculate the $\overline{\omega_{ij}}^1$, $\overline{\varepsilon_{ij}}^1$ by $\bar{u}_i^1$.

Repeat this procedure from (i) to (v) up to the difference between the successive results being less than a definite value.

4. Solution of turbulent fibre suspensions in a pipe flow

4.1. Simplification of equations

The above equations and solutions are applied to the turbulent fibre suspensions in a pipe flow as shown in Fig.1, in which the radius and half-length of each fibre are a and l, respectively. The flow is assumed to be of axial symmetry and fully developed turbulence. The angle included between the fibre's axis and horizontal is θ. In the polar coordinate (r, ϕ, z), Eqs.(9) and (16) can be simplified as



(a) fiber. (b) pipe flow.

Fig.1. Schematic diagram of the fibre and pipe flow.

$$
\begin{aligned}
0 =& -\frac{1}{\rho}\frac{\partial \overline{p}}{\partial r} - \frac{1}{r}\frac{\partial r\overline{u_r'^2}}{\partial r} + \frac{\mu_f}{\rho}\frac{1}{r}\frac{\partial}{\partial r}\left\{ r\left[\overline{a_{rrrz}}\frac{1}{2}\frac{\partial \overline{u}_z}{\partial r} + \overline{a_{rrzr}}\frac{1}{2}\frac{\partial \overline{u}_z}{\partial r} - \frac{1}{3}I_{rr}\left(\overline{a_{rz}}\frac{1}{2}\frac{\partial \overline{u}_z}{\partial r} + \overline{a_{zr}}\frac{1}{2}\frac{\partial \overline{u}_z}{\partial r}\right)\right]\right\},\\
0 =& -\frac{1}{\rho}\frac{\partial \overline{p}}{\partial z} + \nu\left(\frac{\partial^2 \bar{u}_z}{\partial^2 r} + \frac{1}{r}\frac{\partial \bar{u}_z}{\partial r}\right) - \frac{1}{r}\frac{\partial r\overline{u_r' u_z'}}{\partial r}\\
&+ \frac{\mu_f}{\rho}\frac{1}{r}\frac{\partial}{\partial r}\left\{ r\left[\overline{a_{zrrz}}\frac{1}{2}\frac{\partial \overline{u}_z}{\partial r} + \overline{a_{zrzr}}\frac{1}{2}\frac{\partial \overline{u}_z}{\partial r} - \frac{1}{3}I_{zr}\left(\overline{a_{rz}}\frac{1}{2}\frac{\partial \overline{u}_z}{\partial r} + \overline{a_{zr}}\frac{1}{2}\frac{\partial \overline{u}_z}{\partial r}\right)\right]\right\},
\end{aligned}
\tag{19}
$$

and

$$
\begin{aligned}
&-\frac{1}{2}\frac{\partial \overline{u}_z}{\partial r}p_z\frac{\partial \bar{\psi}}{\partial p_r} + \frac{1}{2}\frac{\partial \overline{u}_z}{\partial r}p_r\frac{\partial \bar{\psi}}{\partial p_z} + \lambda\frac{1}{2}\frac{\partial \overline{u}_z}{\partial r}p_z\frac{\partial \bar{\psi}}{\partial p_r} + \lambda\frac{1}{2}\frac{\partial \overline{u}_z}{\partial r}p_r\frac{\partial \bar{\psi}}{\partial p_z}\\
&-\lambda\left(\frac{1}{2}\frac{\partial \overline{u}_z}{\partial r}p_r p_z p_r\frac{\partial \bar{\psi}}{\partial p_r} + \frac{1}{2}\frac{\partial \overline{u}_z}{\partial r}p_z p_r p_r\frac{\partial \bar{\psi}}{\partial p_r}\right) - \lambda\left(\frac{1}{2}\frac{\partial \overline{u}_z}{\partial r}p_r p_z p_z\frac{\partial \bar{\psi}}{\partial p_z} + \frac{1}{2}\frac{\partial \overline{u}_z}{\partial r}p_z p_r p_z\frac{\partial \bar{\psi}}{\partial p_z}\right)\\
&-\lambda\bar{\psi}\left(\frac{1}{2}\frac{\partial \overline{u}_z}{\partial r}p_r p_z + \frac{1}{2}\frac{\partial \overline{u}_z}{\partial r}p_z p_r\right) = \alpha_{\psi x}\left(\frac{\partial^2 \overline{\psi}}{\partial r^2} + \frac{1}{r}\frac{\partial \overline{\psi}}{\partial r}\right) + \alpha_{\psi p}\frac{\partial^2 \overline{\psi}}{\partial p_r^2} + \alpha_{\psi p}\frac{\partial^2 \overline{\psi}}{\partial p_z^2},
\end{aligned}
\tag{20}
$$

where $p_r = \sin\theta$ and $p_z = \cos\theta$.

4.2. Procedure of solving equations

The zero-order approximation solution for the mean velocity of the flow is the mean velocity of the turbulent Newtonian flow without fibre:

$$
\frac{\overline{u}_z(r)}{u^*} = 5.75\ \ \lg\frac{u^*(R-r)}{\nu} + 5.5, \tag{21}
$$

where R is the radius of the pipe, u^* the wall friction velocity and can be calculated by interpolating from $\overline{u}_{av}/u^* = 2.5\ln(u^* R/\nu) + 1.75$, in which $\overline{u}_{av}$ is the mean velocity of the pipe flow. Substituting Eq.(21) into Eq.(20), we can obtain $\bar{\psi}$, then $\overline{a_{ij}}$ and $\overline{a_{ijkl}}$ can be calculated further by solving Eqs.(17) and (18). Finally $\bar{\psi}$, $\overline{a_{ij}}$ and $\overline{a_{ijkl}}$ are inserted into Eq.(20) to obtain the first-order approximation solution for the mean velocity $\bar{u}_i^1$, the turbulent intensity and the Reynolds stress. In the process of deriving the Reynolds stress from Eq.(20), the fluid fluctuating velocities u_r' and u_z' are expanded into the sum of the N simple sine and cosine waves with the Fourier series:

$$
\begin{aligned}
\frac{u_i'(\boldsymbol{x}, t)}{u_{i,\mathrm{rms}}'(\boldsymbol{x})} =& \sum_{n=1}^{N}[(\boldsymbol{b}_n \times \boldsymbol{k}_n)\cos(\boldsymbol{k}_n \cdot \boldsymbol{x} - \omega_n t)\\
&+ (\boldsymbol{c}_n \times \boldsymbol{k}_n)\sin(\boldsymbol{k}_n \cdot \boldsymbol{x} - \omega_n t)],
\end{aligned}
\tag{22}
$$

where N is a large number (N=100 in the paper), $\boldsymbol{b}_n$ and $\boldsymbol{c}_n$ are the vectors composed of Gaussian random numbers, the frequency ω_n is also Gaussian random number whose standard deviation is the RMS (root-mean-square) of the fluctuation velocity $u_{i,\mathrm{rms}}'$, the wave number vector $\boldsymbol{k}_n$ is an isotropic unit random vector. Therefore, the dot product of the coefficient of

primary function and the wave number vector is zero ($(\boldsymbol{b}_n \times \boldsymbol{k}_n) \cdot \boldsymbol{k}_n = 0$) under the condition of continuity for the fluctuation velocity.

5. Experimental set-up and procedure

In order to verify the above equations and their solutions, an experiment for the turbulent pipe flow of fibre suspensions is performed. As shown in Fig.2, the pure water in the tank 1 is pumped to another overflow tank 3 located at a higher position by pump 2. For the sake of maintaining a constant pressure head, the tank 3 is partitioned into two parts by a steel plate. When the water level rises over the top of one part, it will overflow from this part to another part. The flow rate of water can be controlled by the valve 4. The glass fibre suspensions are injected into a pot by a high air pressure, and then flow into the pipe smoothly. The concentration of the fibre mass can be controlled by adjusting the air pressure. The test section 5 is made of a Perspex pip. Before entering the pipe, the fluid passes first through a settling chamber with many screens. There is a disturbed ring 80cm downstream from the settling chamber, which makes the flow fully turbulent as early as possible. The inner diameter of the pipe is 30mm. Due to the difference in the refractive index between the test fluid (water with $n = 1.33$) and the material of the pipe (Perspex with $n = 1.49$), both the change in geometrical parameters of the control volume and the reduction in the sensitivity and spatial resolution of the Laser Doppler Anemometer (LDA) will occur. Therefore, the test section is specially designed as shown in Fig.3, in which the rectangular Perspex box filled with water around the cylindrical pipe will minimize the refraction errors of the laser beams.

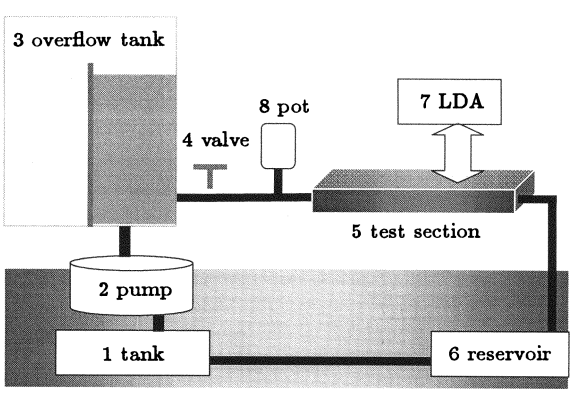


Fig.2. Schematic diagram of experimental set-up.

Before experiment, the glass fibres are cut into small pieces with a length of 1mm, and then injected into the pot 8. The fibres are mixed for 15 minutes in the pot until forming a homogeneous distribution.

In the experiment, firstly, the tank 1 is filled with $1\mathrm{m}^3$ pure water, and meanwhile fibre suspensions with a definite mass concentration are injected into the pot. Secondly, the screw pump is switched on to pump the water from the tank 1 to the tank 3, while keeping the valve 4 closed. Thirdly, the parameters of LDA are adjusted, and the laser beams are focused on the test position. Finally, the valve 4 is switched on, and the pipe flow forms. Before testing, we let the fibre suspensions flow for a while to ensure that the pipe is filled with the fibre suspensions and no bubbles exist in the pipe. The experiments are performed with the different mass concentrations of the fibres. The measured data are processed as the mean velocity, the relative turbulent intensity and the Reynolds stress.

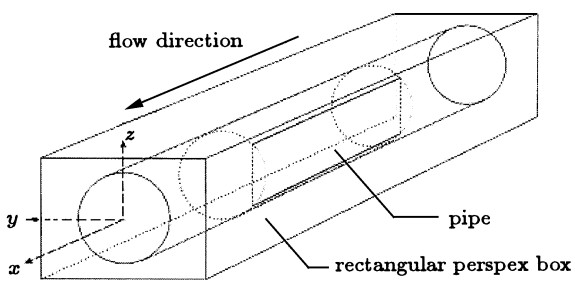


Fig.3. Test section.

6. Results and discussion

6.1. Probability distribution function for mean fibre orientation

The orientation of fibres affects directly the turbulent property of the fibre suspensions. It is difficult, however, to measure the orientation of fibres in a turbulent flow. Bernstein and Shapiro[18] studied experimentally the orientation distribution of the fibres in a turbulent pipe flow of fibre suspensions. The experiment was performed in a pipe whose length and diameter were 4.5m and 38mm, respectively. A microvideo system was used to record the orientation distribution of fibres in a region of 2mm around the pipe center, and the data were analyzed statistically. The probability distribution for angles θ included between the fibre's axis and the horizontal was given. In the present computation, the same parameters as those in that experiment are used to calculate the probability distribution function for fibre orientation in the same

region. A comparison between the computational and experimental results is given in Fig.4. Both results are agreeable with each other.

From Fig.4 we can see that most of the angles included between the fibre's axis and horizontal are small obviously, the maximum of θ is about 10^0. Because the rotation of the fibres results from the velocity gradient of the flow, and the velocity profile near the centre is flat in the turbulent pipe flow, it causes the fibre's axis to tend to the horizontal.

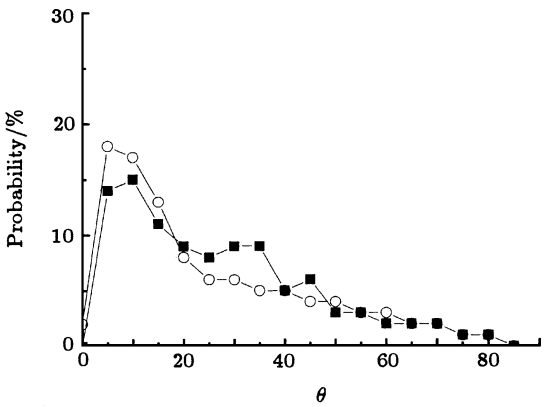


Fig.4. Probability distribution for fibre orientation (Re=11000). —○—: computation; — ■ —: experiment[18].

6.2. Distribution of mean velocity for fibre suspensions

The distribution of mean velocities in the case of different fibre mass concentrations is given in Fig.5, in which the experimental results for the pure water given by Nikuradse[19] are also involved. It can be seen that the computational results are in good agreement with the experimental ones. The velocity profile tends to be flat as the Re number increases, which conforms to the available results. The velocity profile for the fibre suspensions is not so flat as that for the pure water. The pure water flow is similar to the turbulent flow with the same Re number. It illustrates that the fibres suppress the turbulence in the flow. The effect of suppressions is directly proportional to the fibre mass concentration. Figure 6 depicts the mean velocities for the different fibre concentrations. We can see that the mean velocity for the fibre suspensions is larger than that for the pure water, which means that the rate of flow increases. Because the increase in the rate of flow results from the reduction in the drag under the same pressure drop, the fibres play a role in reducing the drag in the flow.

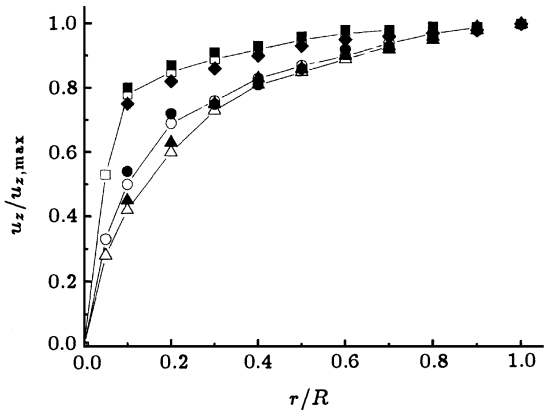


Fig.5. Distribution of the mean velocities. computation (Re=25900): —□—: no fibre, —○—: 2% fibre mass concentration, —△—: 5% fibre mass concentration, experiment (Re=25900): ■: no fibre, ●: 2% fibre mass concentration, ▲: 5% fibre mass concentration, experiment given by Nikuradse[19] (Re=11000): ◆: no fibre.

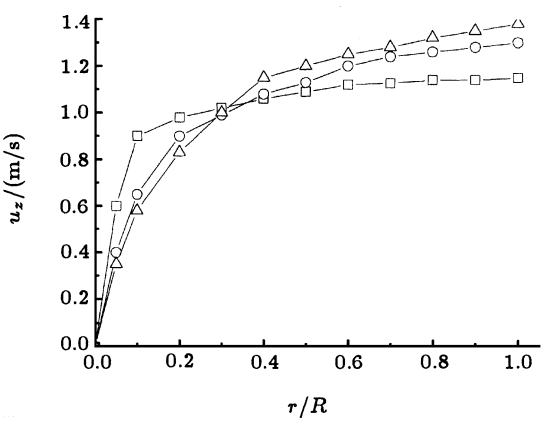


Fig.6. Distribution of mean velocities. computation (Re=25900): —□—: no fibre, —○—: 2% fibre mass concentration, —△—: 5% fibre mass concentration.

6.3. Turbulent intensity and Reynolds stress

The distribution of the streamwise relative turbulent intensities along the radial direction is shown in Fig.7, in which the experimental results given by Laufer[20] are also included. It can be seen that the streamwise relative turbulent intensity augments as Re number increases. The streamwise relative turbulent intensity for the pure water is larger than that for the fibre suspensions. The turbulent intensity decreases with the increase of the fibre mass concentration. It is obvious that the fibres suppress the turbulence. The fact that the streamwise relative turbulent intensity varies with the fibre mass concentration conforms to the feature of the mean velocity profile. Figure 8 depicts the distribution of the radial relative turbulent intensities along the radial direction. We can see that the relative turbulent intensity for the

radial component is smaller than that for the streamwise component. The effects of the fibres on the radial and streamwise relative turbulent intensities are the same. Figure 9 shows the distribution of the Reynolds stresses along the radial direction. It can be seen that the fibres suppress the Reynolds stress in the flow, and effect of suppression is directly proportional to the fibre mass concentration.

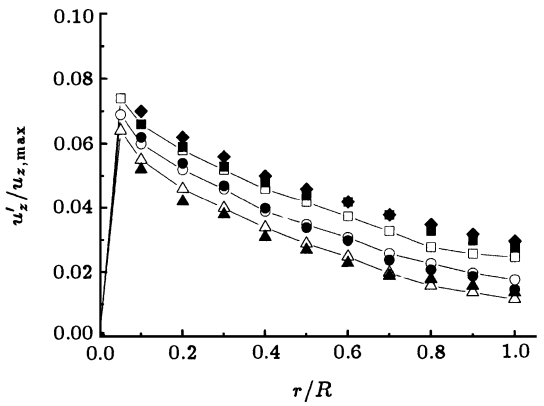


Fig.7. Distribution of streamwise relative turbulent intensities along the radial direction. computation (Re=25900): —□—: no fibre, —○—: 2% fibre mass concentration, —△—: 5% fibre mass concentration, experiment (Re=25900): ■: no fibre, ●: 2% fibre mass concentration, ▲: 5% fibre mass concentration, experiment given by Laufer[20] (Re=50000): ◆: no fibre.

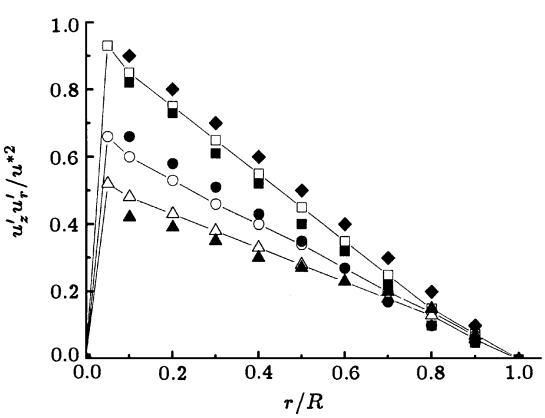


Fig.8. Distribution of radial relative turbulent intensities along the radial direction. computation (Re=25900): —□—: no fibre, —○—: 2% fibre mass concentration, —△—: 5% fibre mass concentration, experiment (Re=25900): ■: no fibre, ●: 2% fibre mass concentration, ▲: 5% fibre mass concentration, experiment given by Laufer[20] (Re=50000): ◆: no fibre.

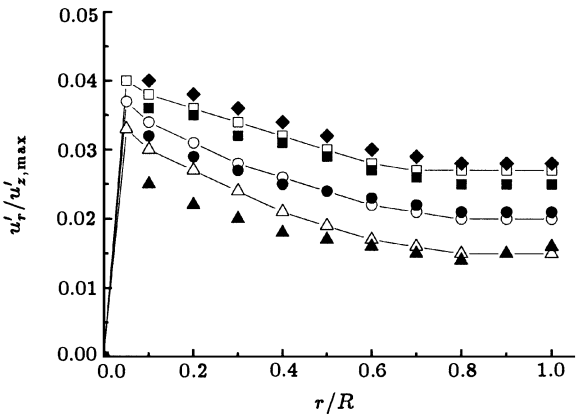


Fig.9. Distribution of Reynolds stresses along the radial direction. computation (Re=25900): —□—: no fibre, —○—: 2% fibre mass concentration, —△—: 5% fibre mass concentration, experiment (Re=25900): ■: no fibre, ●: 2% fibre mass concentration, ▲: 5% fibre mass concentration, experiment given by Laufer[20] (Re=50000): ◆: no fibre.

7. Conclusion

Based on the instantaneous motion equation of fibre suspensions and the equation of probability distribution function for fibre orientation, derived are the equation of mean motion, which includes the Reynolds stress and the effect of the fibres, and the equation of probability distribution function for mean fibre orientation, which includes the fluctuating correlation. A successive iteration of solving the above equations is presented. The equations and their solutions are proved to be correct and feasible by applying them to a turbulent pipe flow of fibre suspensions and by comparing the computational results with the experimental ones. The obtained results show that under the same condition, the rate of flow for the fibre suspensions is larger than that for the pure water, and the relative turbulent intensity and the Reynolds stress for the fibre suspensions, however, are smaller than those for the pure water. Therefore, the fibres in the flow play a role in suppressing the turbulence and reducing the drag, such effects become more obvious with the increase of the fibre mass concentration.

References

[1] Asgharian B and Yu C 1989 *J. Aerosol Sci.* **30** 355

[2] Kagermann H and Kohler W 1984 *Physica* A **116** 178

[3] Krushkal E and Gallily I 1988 *J. Aerosol Sci.* **19** 197

[4] Olson J A and Kerekes R J 1998 *J. Fluid Mech.* **377** 47

[5] Olson J A 2001 *Int. J. Multiphase Flow* **27** 2083

[6] Lin J Z, Shi X and Yu Z S 2003 *Int. J. Multiphase flow*

29 1355
[7] Lin J Z, Zhang W F and Yu Z S 2004 *J. Aerosol Sci.* **35** 63
[8] Gao Z Y and Lin J Z 2004 *J. Hydrodynam.* **16** 1
[9] Lin J Z, Lin J and Shi X 2002 *Appl. Math. Mech.* **23** 542
[10] Batchelor G K 1971 *J. Fluid Mech.* **46** 813
[11] Zhao H P, Liu Z Y and Liu Y Y 2001 *Chin. Phys.* **10** 35
[12] Zhao X P and Gao D 2001 *Acta Phys. Sin.* **50** 1115 (in Chinese)
[13] Li H B and Fang H P 2004 *Chin. Phys.* **13** 2087
[14] Shaqfeh E S G and Fredrickson G H 1990 *Phys. Fluids* A **2** 7
[15] Hinch E J and Leal L G 1976 *J. Fluid Mech.* **76** 187
[16] Advani S G and Tucke C L 1987 *J. Rheol.* **31** 751
[17] Cintra J S and Tucker C L 1995 *J. Rheol.* **39** 1095
[18] Bernstein O and Shapiro M 1994 *J. Aerosol Sci.* **25** 113
[19] Nikuradse J 1933 *Arb. Ing. Wes.* **361** 353
[20] Laufer J 1954 *Tech. Repts.* **1174** 417